

Constraining light dark matter and mediator with $B^+ \rightarrow K^+ \nu \bar{\nu}$ data

Murat Abdughani^{*} and Yakefu Reyimuaji[†]

School of Physical Science and Technology, Xinjiang University, Urumqi 830017, China

 (Received 26 January 2024; accepted 19 August 2024; published 9 September 2024)

We study the decay of B^+ meson into K^+ plus a light mediator ϕ , which subsequently decays into a dark matter pair, $\bar{\chi}\chi$. Integrating constraints from DM relic density, direct detection, collider data and B -physics, alongside the recently reported results from Belle II experiment, we analyze the couplings between the mediator, standard model fermions, and the dark matter particles. Our results indicate that if the decay process $\phi \rightarrow \bar{\chi}\chi$ is kinematically allowed, i.e., $m_\phi > 2m_\chi$, then the mediator mass must be constrained within $0.35 \text{ GeV} \lesssim m_\phi \lesssim 3 \text{ GeV}$. Conversely, if $m_\phi < 2m_\chi$, the mediator m_ϕ is long-lived relative to the detector size, and the only allowed decay channel is $\phi \rightarrow e^+e^-$.

DOI: [10.1103/PhysRevD.110.055013](https://doi.org/10.1103/PhysRevD.110.055013)

I. INTRODUCTION

Rare B -meson decay with a kaon and neutrino pair in the final state, i.e., $B^+ \rightarrow K^+ \nu \bar{\nu}$, has a clear theoretical prediction among the flavor changing neutral current processes. It is severely suppressed due to the loop effect and the Glashow-Iliopoulos-Maiani mechanism [1]. Thus, it plays an important role in searching for new physics and testing the Standard Model (SM). While the SM prediction for the branching fraction is $(5.58 \pm 0.37) \times 10^{-6}$ [2], the Belle II experiment at the SuperKEKB asymmetric energy electron-positron collider has recently reported the value of $(2.3 \pm 0.7) \times 10^{-5}$ [3] with the significance of about 3σ above the SM prediction. This discrepancy may call for the new physics beyond the SM (BSM).

Although the weak interaction of neutrinos makes it invisible at the detector, processes with missing energy \cancel{E} in the final state, i.e., $B^+ \rightarrow K^+ + \cancel{E}$, may not contribute to measured branching fraction of the decay $B^+ \rightarrow K^+ \nu \bar{\nu}$ in Ref. [3]. This decay process can be reinterpreted to the two-body decay process $B^+ \rightarrow K^+ X$ [4], where X is stable or decay invisibly. In this interpretation, they achieved maximum branching ratio of $\text{Br}[B^+ \rightarrow K^+ X] = (8.8 \pm 2.5) \times 10^{-6}$ with a significance of 3.8σ at $m_X \simeq 2 \text{ GeV}$. Considering the no excess in BABAR experiment, the combined result is $\text{Br}[B^+ \rightarrow K^+ X] = (5.1 \pm 2.1) \times 10^{-6}$ with a significance of 2.4σ . Similar two-body decay processes have also been studied at Refs. [5,6]. Dark matter (DM) or any other light

particles with sufficiently weak interaction strength involved in this process can be considered as the missing energy. Therefore, precision experiments of B meson decay are crucial in the searching or constraining the DM and other light BSM particles.

DM on the other side, is an indispensable ingredient for the evolution of the Universe. The thermal DM known to be in equilibrium with SM particles in the early times and freeze-out later when its annihilation rate could not catch up with the expansion rate of the Universe [7]. After the thermal freeze-out, the DM comoving number density remains constant and leads to the observed DM relic abundance. This, on the other hand, determines the DM annihilation rate at the freeze-out. Interestingly, annihilation cross section of this process is of the same order of magnitude as the weak interaction. Thus, this weakly interacting massive particle (WIMP) [8] has become the mostly well-studied and promising candidate for DM. The lower limit for the mass of the WIMP, which is model dependent, is conventionally a few GeV [9]. However, the null result from various DM search experiments have pushed the lower limit to MeV scale with proper parameter or model selection [10].

Combined study of DM and new physics hint from B -meson decay is an intriguing window towards the construction of BSM physics. In this work, an extension of the SM with a light scalar mediator and a Majorana fermion is studied. By integrating constraints from various experiments, we delineate the optimal parameter ranges for our model. The paper is structured as follows. In Sec. II a simple DM model is presented. Section III gives discussions about the B -meson decay into kaon and SM fermions as well as extra fermionic DM pairs. Experimental constraints and parameter spaces are studied in Sec. IV, followed by results and discussions in Sec. V. Finally, the conclusion of the paper is drawn in Sec. VI.

^{*}Contact author: mulati@xju.edu.cn

[†]Contact author: yreyi@hotmail.com

Published by the American Physical Society under the terms of the Creative Commons Attribution 4.0 International license. Further distribution of this work must maintain attribution to the author(s) and the published article's title, journal citation, and DOI. Funded by SCOAP³.

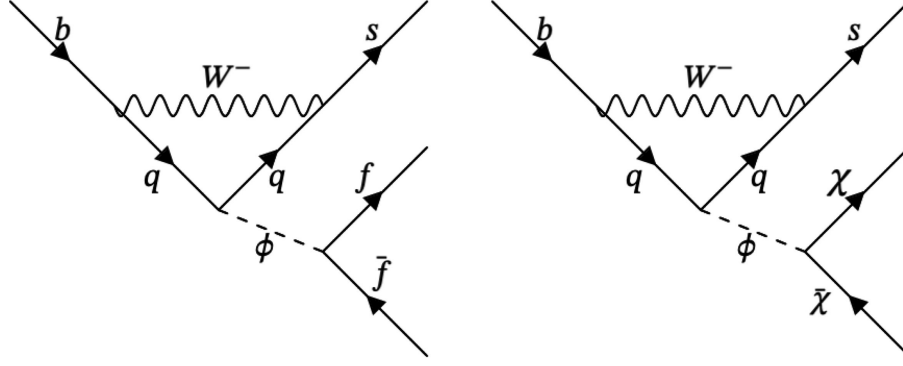


FIG. 1. The BSM leading-order Feynman diagrams for $b \rightarrow s\chi\bar{\chi}$ and $b \rightarrow sf\bar{f}$ processes. The q stands for u, c, t quarks, f include all quarks and massive leptons.

II. A SIMPLE DM MODEL

In this section, we study a generic model featuring light Majorana DM χ and a light scalar ϕ that couples with the SM fermions. The dimension-4 interaction Lagrangian can be simply written as¹

$$\mathcal{L}_{\text{int}} = -\frac{ym_f}{v}\phi\bar{f}f - \frac{1}{2}\kappa\phi\bar{\chi}\chi, \quad (1)$$

where m_f represent the masses of the SM fermions, y is the weight of the Yukawa coupling, $v \simeq 246$ GeV is the electroweak vacuum expectation value. The Feynman diagrams at the leading-order for DM and fermion pair productions in the final state are illustrated in Fig. 1.

We note that the simple Lagrangian in Eq. (1) does not originate from gauge symmetry but is phenomenologically viable after the electroweak symmetry breaking of higher-dimensional effective operators [13]. The constant $\frac{m_f}{v}$ in the coupling indicates that this operator is induced from integrating out the Higgs portal [14]. Effective field theory approaches to the decay processes of B meson with a single invisible scalar or fermion pair in the final state in dimension-5 or dimension-6 operators have been studied in Refs. [11,12,15–18]. The anomaly is also explained by the UV complete models [19–21].

III. B-MESON DECAY

When the scalar mediator mass, m_ϕ , is smaller than the mass difference between the B and K meson, i.e., $m_\phi < m_B - m_K$, the effective Lagrangian for the $b \rightarrow s\phi$ process can be obtained by integrating out heavy particles running in the loop shown in the Fig. 1. This process is described by the following Lagrangian [22,23]:

¹Pseudoscalar current $\bar{f}\gamma^5 f$ vanishes at the loop order for $0^- \rightarrow 0^-$ meson decay processes [11,12].

$$\mathcal{L}_{b \rightarrow s\phi} = \frac{ym_b}{v} \frac{3\sqrt{2}G_F m_q^2 V_{qs}^* V_{qb}}{16\pi^2} \times \phi \bar{s}_L b_R + \text{H.c.}, \quad (2)$$

where q denotes the u, c, t quarks in the loop, G_F is the Fermi constant, and $V_{qs,qb}$ are the Cabibbo-Kobayashi-Maskawa (CKM) matrix elements. It is obvious that contribution from the quarks other than the top are negligible.

The decay width for the process $B \rightarrow K + \phi$ is given by

$$\begin{aligned} \Gamma_{B \rightarrow K\phi} &= \left(\frac{ym_b}{v} \frac{3\sqrt{2}G_F m_q^2 V_{ts}^* V_{tb}}{16\pi^2} \right)^2 \\ &\times \frac{\sqrt{(m_B^2 - (m_K + m_\phi)^2)(m_B^2 - (m_K - m_\phi)^2)}}{16\pi m_B^3} \\ &\times |\langle K | \bar{s}_L b_R | B \rangle|^2, \end{aligned} \quad (3)$$

where the hadronic transition matrix element is

$$\langle K | \bar{s}_L b_R | B \rangle = \frac{m_B^2 - m_K^2}{2(m_b - m_s)} f_0(q^2), \quad (4)$$

and $m_{b,s}$ are the masses of the bottom and strange quark, respectively. The $f_0(q^2)$ is the form factor, with $q^2 = m_\phi^2$ for the final-state particle ϕ . We adopted two different form factor schemes from Refs. [24] and [25] for the stability of our result, and details of which are discussed in the Appendix. Our analysis reveals that the results obtained from two schemes are merely distinguishable; hence, we present only the results from the first scheme in the main text.

Subsequently, if kinematically allowed, the scalar ϕ may decay into DM or SM fermion pairs. The decay width of ϕ to a fermion pair, including DM, is

$$\Gamma_{\phi \rightarrow \bar{f}f} = \frac{C_{\phi\bar{f}f}^2}{8\pi} m_\phi \left(1 - \frac{4m_f^2}{m_\phi^2} \right)^{3/2} \Theta(m_\phi - 2m_f), \quad (5)$$

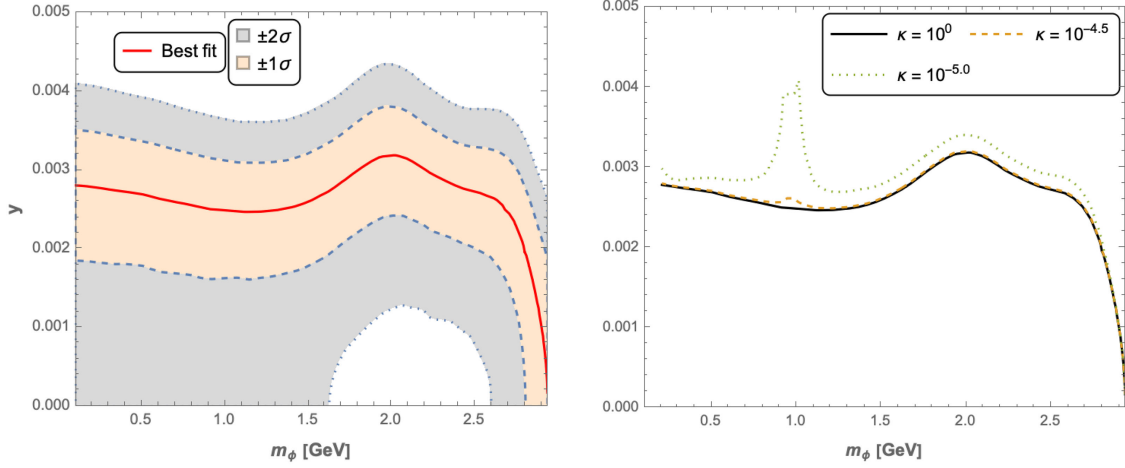


FIG. 2. Left: best-fit line (red solid line), with 1σ (light yellow) and 2σ (light gray) shaded areas, satisfying the branching fraction of $B \rightarrow K + \phi$ as shown in Fig. 1 of Ref. [4] in (m_ϕ, y) space. Right: the branching fractions of process $B \rightarrow K + \phi$ followed by $\phi \rightarrow \bar{\chi}\chi$ align with the best-fit line in the left panel for different κ values, where DM masses are fixed at 0.1 GeV.

where $C_{\phi\bar{f}f}^2$ is scalar-fermion-fermion interaction coefficient, and Θ is the Heaviside step function. For the decay width to the hadronic final states, we consulted to the Refs. [15,22,26].

In the left panel of Fig. 2, we show the coupling y as a function of m_ϕ , adopting the branching fraction of $B \rightarrow K + \phi$ from Fig. 1 of Ref. [4], assuming that branching fraction of ϕ decays into $\chi\bar{\chi}$ is 100%. In the right panel, with m_χ fixed at 0.1 GeV, we draw curves for different κ values that achieve the same branching ratios as the red solid line in the left panel. For the fixed m_χ and m_ϕ , as the value of κ decreases, the branching fraction $\text{Br}[\phi \rightarrow \bar{\chi}\chi]$ also decreases. Consequently, a larger y is required to increase $\text{Br}[B \rightarrow K + \phi]$ so that the overall $\text{Br}[B \rightarrow K + \bar{\chi}\chi] \equiv \text{Br}[B \rightarrow K + \phi] \times \text{Br}[\phi \rightarrow \bar{\chi}\chi]$ aligns with the desired values. The bump near $m_\phi \sim 1$ GeV is due to the peak in the decay width to SM particles shown as in Fig. 4 of Ref. [15], which is caused by a pion pair in the final state.

IV. DM RELIC DENSITY AND CONSTRAINTS

When the decay process $\phi \rightarrow \bar{\chi}\chi$ is kinematically allowed, that is, $m_\chi < m_\phi/2$, in the vicinity of freeze-out, DM can only annihilate into lighter SM fermion pairs through an s -channel heavy mediator ϕ . The cross section which determines the DM relic density for the process $\bar{\chi}\chi \rightarrow \bar{f}f$ is given by

$$\sigma_{\bar{\chi}\chi \rightarrow \bar{f}f} = \frac{1}{512\pi} \left(\frac{\kappa y m_f}{v} \right)^2 \sqrt{1 - \frac{4m_f^2}{s}} \left(1 - \frac{2m_f^2}{s} \right) \times \left(1 - \frac{2m_\chi^2}{s} \right) \frac{s}{(s - m_\phi^2)^2}, \quad (6)$$

where $s \equiv E_{\text{cm}}^2$ is the center-of-mass energy squared. Note that this equation holds for nonresonant annihilation. The thermally averaged cross section is defined as [27]

$$\langle \sigma v \rangle_{\bar{\chi}\chi \rightarrow \bar{f}f} = \int_{4m_\chi^2}^{\infty} ds \sigma_{\bar{\chi}\chi \rightarrow \bar{f}f} \times v_{\text{lab}} \frac{\sqrt{s - 4m_\chi^2} (s - 2m_\chi^2) K_1(\sqrt{s}/T)}{8m_\chi^4 T K_2^2(m_\chi/T)}, \quad (7)$$

where K_i are the modified Bessel functions of order i . If DM does not resonantly annihilate, the possible maximum of $\langle \sigma v \rangle$ is at least three orders less than the standard thermal cross section of $10^{-26} \text{ cm}^3/\text{s}$. Therefore, we have to resort to resonantly enhanced cross section of DM annihilation. We utilize FeynRules [28] to implement the models, and then import them to micrOMEGAS-5.3.41 [29] for the calculation of DM relic density and DM-nucleus cross section.

To explore full parametric phase space, we scan over the range specified in Table I, where upper limit of 0.1 for y is taken from LEP [30]. We evaluate the likelihoods associated with DM relic density measurements from Planck and direct detection (DD) results from various experiments. The χ_{scan}^2 is defined as the sum of the individual χ^2 values from the DM relic density and the DD processes,

$$\chi_{\text{scan}}^2 = \chi_{\Omega h^2}^2 + \chi_{\text{DD}}^2. \quad (8)$$

We hire emcee [31] based on Markov chain Monte Carlo (MCMC) method to undertake the task of sampling the parameter space with the likelihood $\propto \exp(-\chi_{\text{scan}}^2/2)$.

The χ^2 of DM relic density is described by the Gaussian distribution,

TABLE I. Ranges and priors for input parameters adopted in the scans.

Parameters	Minimum	Maximum	Prior
m_ϕ	0.01 GeV	$m_B - m_K$	Flat/log
m_χ	0.01 GeV	$m_\phi/2$	Flat/log
κ	10^{-6}	4	log
y	10^{-6}	0.1	log

$$\chi_{\Omega h^2}^2 = \left(\frac{\mu_t - \mu_0}{\sqrt{\sigma_{\text{theo}}^2 + \sigma_{\text{exp}}^2}} \right)^2, \quad (9)$$

where μ_t is the predicted theoretical value we obtained, and μ_0 is the experimental central value. We introduce a 10% theoretical uncertainty, $\sigma_{\text{theo}}^2 = 0.1\mu_t$, to account for uncertainties from the Boltzmann equation solver and the entropy table in the early Universe. The predicted relic density Ωh^2 is constrained using the Planck 2018 data [32], which reports a central value with statistical error as $\Omega h^2 = 0.118 \pm 0.002$.

The estimation of χ^2 for the DM-nucleus spin-independent and spin-dependent cross section is given by

$$\chi_{\text{DD}}^2 = \left(\frac{\sigma_{\text{DD}}}{\sigma_{\text{DD}}^0/1.64} \right)^2, \quad (10)$$

where σ_{DD} represents the predicted theoretical value obtained from micrOMEGAs-5.3.41, and σ_{DD}^0 denotes the upper limits of the cross sections for a given DM mass at the 90% confidence level. These limits are provided by experiments such as DarkSide-50 [33], CRESST-III [34], PICO-60 [35], PandaX-4T [36], and Xenon1T [37].

Apart from the constraints from relic density and DD implemented during the scanning process, we also considered following phenomenological implications of the model which may challenge the possible surviving phase space:

- (i) The model [Eq. (1)] also generates processes like $b \rightarrow d\phi$ and $s \rightarrow d\phi$, which contribute to $B^0 \rightarrow \text{invisible}$, $B^+ \rightarrow \pi^+ \cancel{E}$, and $K^+ \rightarrow \pi^+ \cancel{E}$, by changing the appropriate quark fields, CKM matrix elements or form factors.

Although matrix element $\langle 0 | \bar{b}d | B \rangle$ vanishes [38], $\langle 0 | \bar{b}\gamma_5 d | B \rangle = -i \frac{f_B m_B^2}{m_b + m_d}$ contribute to the decay width of the process $B^0 \rightarrow \text{invisible}$, which is

$$\Gamma_{B^0 \rightarrow \chi\bar{\chi}} \simeq \left(\frac{y\kappa G_F m_t V_{td}^* V_{tb}}{v} \right)^2 \frac{f_B^2 m_B^5}{16\pi(m_b + m_d)^2} \times \sqrt{1 - \frac{4m_\chi^2}{m_B^2} \frac{1}{(m_B^2 - m_\phi^2)^2}}. \quad (11)$$

When $2m_\chi = m_\phi < 3$ GeV and $\kappa = 1$, branching ratio is $\text{Br}[B^0 \rightarrow \text{invisible}] \lesssim 3.8 \times 10^{-5} y^2$. Therefore, the experimental upper limit $\text{Br}[B^0 \rightarrow \text{invisible}] < 7.8 \times 10^{-5}$ [39] is easily satisfied.

For the process $B^+ \rightarrow \pi^+ \phi$, the corresponding decay width can be obtained by substituting the CKM matrix elements V_{ts} with V_{td} and replacing the kaon mass m_K with and pion mass m_π in Eq. (3). Given that $V_{td} \simeq 0.2V_{ts}$ [40], the decay width $\Gamma_{B \rightarrow \pi\phi}$ is approximately $0.04\Gamma_{B \rightarrow K\phi}$. Since the experimental upper limit $\text{Br}[B^+ \rightarrow \pi^+ \cancel{E}] < 6.4 \times 10^{-6}$ [41] is comparable to $\text{Br}[B^+ \rightarrow K^+ \phi]$, the $B^+ \rightarrow \pi^+ \phi$ process does not impose additional constraints.

Similarly, the decay width for $K^+ \rightarrow \pi^+ \phi$ is determined by replacing V_{tb} , bottom quark mass m_b , m_B , m_K , and the form factor $f_0(q^2)$ with V_{td} , strange quark mass m_s , m_K , m_π and the $K \rightarrow \pi$ form factor $f_0^{K^+}(q^2)$, respectively. The form factor $f_0^{K^+}(q^2) = f_0^{K^+}(0)(1 + \lambda_0 q^2/m_\pi^2)$, where $f_0^{K^+}(0) = 0.9778$ and $\lambda_0 = 0.01338$ [42,43]. For a $y \sim 10^{-3}$, the branching ratio $\text{Br}[K^+ \rightarrow \pi^+ \phi]$ is at the order of 10^{-6} , which significantly exceeding the experimental upper limit of $\text{Br}[K^+ \rightarrow \pi^+ \cancel{E}] \lesssim 10^{-11}$ [44]. Therefore, m_ϕ should not be lighter than $m_K - m_\pi$, as illustrated in the gray shaded region of Fig. 3.

- (ii) The scalar mediator ϕ couple to the all SM fermions, thereby influencing rare leptonic decays such as $b \rightarrow (s, d)l^+l^-$ and $s \rightarrow dl^+l^-$, $l = e, \mu$. Additionally, hadronic decays like $b \rightarrow (s, d)q\bar{q}$ and $s \rightarrow dq\bar{q}$ can also constrain the parameter space. Several studies have investigated the decay of scalar

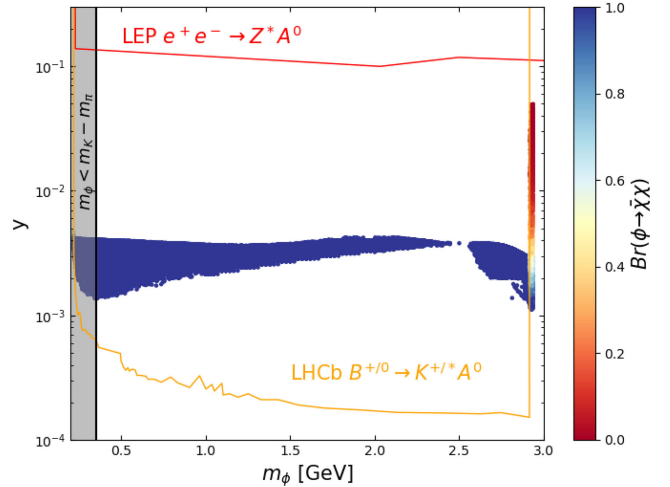


FIG. 3. Survived sample points with the constraints $\chi_{\text{tot}}^2 < 6$ and $\text{Br}[B \rightarrow K + \bar{\chi}\chi] < 2\sigma$. The colorbar represents the branching fraction of $\phi \rightarrow \bar{\chi}\chi$ process. The red and orange solid lines are the upper limits of experimental constraints from LEP [30] and LHCb [52,53], respectively. The gray shaded region is excluded by $\text{Br}[K^+ \rightarrow \pi^+ \phi]$ data.

mediators to SM fermion pairs [15,45–49], providing constraints on the coupling parameter as a function of m_ϕ . These constraints are critical in defining the viable parameter space of our model.

A distinct aspect of this paper, compared to previous works, is that the branching fraction of ϕ decay to all possible SM particles, denoted as $\text{Br}(\phi \rightarrow \text{SM SM})$, is not necessarily unity. Consequently, we must adjust the limits derived from experiments such as LEP [30], Belle [50], BESIII [51], LHCb [52,53], NA62 [44,54,55], KTeV [15,56,57], CHARM [15,45,58–60], and PS191 [61]. If we posit $\text{Br}(\phi \rightarrow \text{SM SM}) = f_{\text{SM}}$ for a specific parameter set where $y = y_0$ and other parameters are fixed, the equivalent y should be recalculated as

$$y' = (y_0^4 / f_{\text{SM}})^{1/4}, \quad (12)$$

assuming that SM particles are the sole decay products. Therefore, the exclusion limits becomes more robust if the branching fractions to the SM final states are less than one.

The estimation of χ^2 for the y can be analogized to the expression for χ_{DD}^2 given by Eq. (10). By integrating the relationship defined in Eq. (12), we can formulate χ_y^2 as follows:

$$\chi_y^2 = \left(\frac{y}{f_{\text{SM}}^{1/4} y^{90\%} / 1.64} \right)^2, \quad (13)$$

where y represents the coupling parameter at our sample points, and $y^{90\%}$ denotes the experimental upper limits of y for a given m_ϕ at the 90% confidence level from the referenced experiments. This formulation ensures that χ_y^2 captures the maximum deviation of the observed coupling from its experimental limits, weighted by the branching fraction to SM particles.

In Fig. 3, we present two primary constraint lines from LEP [30] and LHCb [52,53]. These constraints rule out ($\chi_y^2 > 4$) the sample points with SM final states, thereby only the DM final decay processes are survived in this region.

- (iii) The model generates decaying channels of Higgs and weak bosons at the tree level if kinematically allowed, $H/Z \rightarrow f\bar{f}\phi$ and $W \rightarrow f\bar{f}'\phi$, as well as the top-quark decay $t \rightarrow bW\phi$. However, these tree-level diagrams are significantly suppressed by a factor of about $(\frac{ym_t}{v})^2$. Given that the largest possible value for m_f in this factor is the mass of bottom quark, and considering $y \simeq 10^{-3}$, the contributions from these processes to the decay widths of H , Z , W , and t are negligible.

- (iv) Additionally, our model also generates Higgs and Z-boson invisible decays at the one loop level, $H \rightarrow \phi\phi$ and $Z \rightarrow \phi\phi$. The suppression for these decay processes can be quantified as approximately $(\frac{ym_t}{v} \frac{m_t}{m_b})^2 \frac{1}{m_H^4}$ for the Higgs and $(\frac{ym_t}{v})^2 \frac{1}{m_Z^4}$ for the Z boson. These suppression factors render the contributions to the decay widths significantly smaller than the experimental uncertainties associated with these processes.

V. RESULTS AND DISCUSSION

In the Fig. 3, we present sample plots where total χ^2 value, $\chi_{\text{tot}}^2 = \chi_{\text{scan}}^2 + \chi_y^2$, is less than 6, with the minimum value of $\chi_{\text{tot}}^2 \simeq 0$. These plots also ensure that the branching fraction $\text{Br}[B \rightarrow K + \bar{\chi}\chi]$ falls within the 2σ range. The relevant constraint lines from LEP [30] and LHCb [52,53] are also shown. It is evident from the figure that, in regions above the experimental upper limits, the branching fraction to the DM pair must be very close to one for these sample points to survive.

SM final state particles can be part of ϕ decay channels below the experimental exclusion lines. The closer to the upper limit, the bigger $\text{Br}[\phi \rightarrow \text{SM SM}]$ gets as indicated in Eq. (12). These sample points with nonzero $\text{Br}[\phi \rightarrow \text{SM SM}]$ are located at the charmonium resonant area. Actually, this narrow resonance area was vetoed by excluding the region to avoid contamination, and no search is performed in the original Ref. [52].

There is no sample point survive when $m_\phi \lesssim 2m_\mu$, since where only $\bar{\chi}\chi \rightarrow e^+e^-$ channel allowed and corresponding annihilation cross section is too small even if one introduces the resonant enhancement. However, constraint from $\text{Br}[K^+ \rightarrow \pi^+\phi]$ data is even stronger, and push the lower limit of m_ϕ to the $m_k - m_\pi$. When annihilation process $\bar{\chi}\chi \rightarrow \bar{c}c$ is closed, DM relic density is on the high side, and that is the reason why there is a gap near $m_\phi \simeq 2.5$ GeV.

Note that if the lifetime of ϕ particle is long enough to escape from the detector before decaying, ϕ acts as the missing energy regardless of the decay products. However, to match with DM relic density and $\text{Br}[B \rightarrow K + \phi]$, both κ and y can not be too small. In our sample points in Fig. 3, maximum lifetime of the ϕ particle is of the order of $\sim 10^{-14}$ s, thus it can be seen as prompt decay in the detector. For the long-lived ϕ and displaced vertex, one can resort to the Refs. [15,17,49], where the exclusion capability may differ.

On the other hand, if $m_\gamma > m_\phi/2$, although the decay products of ϕ are only the SM particles, long-lived ϕ relative to the detector size behaves like missing energy. When $y \simeq 3 \times 10^{-3}$ and $m_\phi < 2m_\mu$, the decay width $\Gamma(\phi \rightarrow e^+e^-)$ can be less than 10^{-15} GeV to be invisible. Additionally, m_ϕ must be heavier than electron pair mass to ensure decay prior to the big bang nucleosynthesis. In this

scenario, heavy DM can easily satisfy the observed relic density [15,45]. Such a DM with light scalar mediator that satisfies the B -meson anomaly constraints is predicted to have a sizable direct detection cross section [62,63], and this makes it ready to test in the near future experiments.

VI. CONCLUSION

In this paper, we have explored a simple model involving a light mediator ϕ and a light DM particle χ , inspired by the reinterpretation of recent Belle II results from the $B \rightarrow K + \bar{\nu}\nu$ measurement into the two-body decay $B \rightarrow K + \phi$. Through a comprehensive analysis of the parameter space, supported by experimental results, we have identified that when $2m_\chi < m_\phi$ —allowing for the decay $\phi \rightarrow \bar{\chi}\chi$ —the mass of ϕ must be heavier than that of the muon pair. Moreover, constraints from the $\text{Br}[K^+ \rightarrow \pi^+\phi]$ data extend the lower mass limit of ϕ to approximately 0.35 GeV, equivalent to $m_K - m_\pi$. In addition, the branching fraction of ϕ to the DM pair must be very close to the one to escape the constraints from LHCb, except in a narrow region near $m_\phi \simeq 3$ GeV, where ϕ can decay to SM particles partially. When $m_\chi > m_\phi/2$, DM easily have correct relic density, ϕ should play the role of missing energy in the detector, and small width of ϕ requires $m_\phi < 2m_\mu$. In other word, ϕ can only decay to electron pair. The model in this work is rather simple and includes small number of parameters, and its predictions are within the reach of current or near future experiments, which increases testability of the model.

ACKNOWLEDGMENTS

M. A. is supported by the National Natural Science Foundation of the People's Republic of China (No. 12303002) and Xinjiang Tianchi Doctoral Project of Xinjiang Uygur autonomous region of China. Y. R. is supported by the Natural Science Foundation of Xinjiang Uygur Autonomous Region of China under Grant No. 2022D01C52.

APPENDIX: $B \rightarrow K$ FORM FACTORS

We adopted two different form factor schemes for the stability of our result. The first one is from Ref. [24], which is the combination of latest lattice result from Ref. [64] and the previous lattice one in Ref. [65]. The second one is outlined in Ref. [25], which is the combination of Ref. [64] with the latest light cone sum rule result of Ref. [66].

(1) In Ref. [24], parametrization for the $B \rightarrow K$ form factor is from FLAG [67],

$$f_0(q^2) = \frac{1}{1 - q^2/M_0^2} [a_0 + a_1 z(q^2)], \quad (\text{A1})$$

with $M_0 = 5.711$ GeV, and

TABLE II. Fit results of the coefficients with uncertainties and the correlation matrix [25].

a_0	a_1	a_2
0.3233(67)	0.214(57)	-0.12(13)
	0.8083	0.5481
		0.9074

$$z(q^2) = \frac{\sqrt{t_+ - q^2} - \sqrt{t_+ - t_0}}{\sqrt{t_+ - q^2} + \sqrt{t_+ - t_0}}, \quad (\text{A2})$$

where $t_+ = (m_B + m_K)^2$ and $t_0 = (m_B + m_K)(\sqrt{m_B} - \sqrt{m_K})^2$. Coefficients a_0 , a_1 , and their correlation matrix element are 0.2939(36), 0.227(40), and 0.4568, respectively.

(2) In Ref. [25], they adopted parametrization [68]

$$f_0(q^2) = \frac{1}{1 - q^2/M_0^2} [a_0 + a_1(z(q^2) - z(0)) + a_2(z(q^2) - z(0))^2], \quad (\text{A3})$$

with coefficients and correlation matrix are given as in Table II.

For a quantitative comparison between two form factor schemes described above, we draw the Fig. 4. The gap between two schemes become larger for small m_ϕ , but relative difference at most about 3% as shown in the lower panel. The 1σ uncertainty range for the form factors are very narrow. For the clear illustration, enlarged a small area near $m_\phi \sim 2$ GeV for the first form factor scheme.

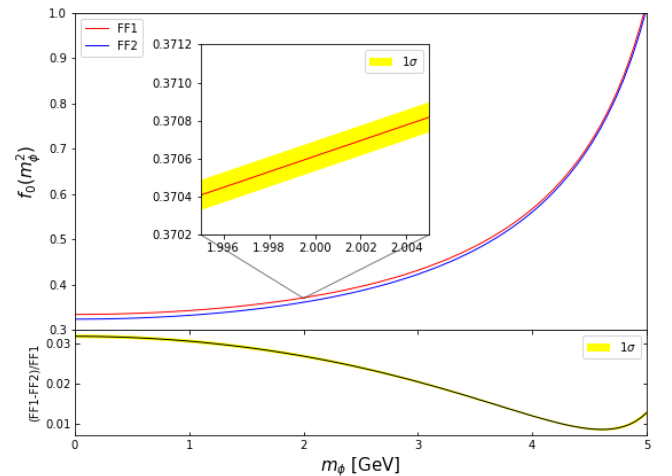


FIG. 4. The form factors and relative differences as a function of m_ϕ . FF1 is for the fitted results from Ref. [24], while FF2 is for the Ref. [25].

- [1] S. L. Glashow, J. Iliopoulos, and L. Maiani, *Phys. Rev. D* **2**, 1285 (1970).
- [2] W. G. Parrott, C. Bouchard, and C. T. H. Davies (HPQCD Collaboration), *Phys. Rev. D* **107**, 014511 (2023); **107**, 119903(E) (2023).
- [3] I. Adachi *et al.* (Belle-II Collaboration), *Phys. Rev. D* **109**, 112006 (2024).
- [4] W. Altmannshofer, A. Crivellin, H. Haigh, G. Inguglia, and J. Martin Camalich, *Phys. Rev. D* **109**, 075008 (2024).
- [5] J. Martin Camalich, M. Pospelov, P. N. H. Vuong, R. Ziegler, and J. Zupan, *Phys. Rev. D* **102**, 015023 (2020).
- [6] T. Ferber, A. Filimonova, R. Schäfer, and S. Westhoff, *J. High Energy Phys.* 04 (2023) 131.
- [7] M. Srednicki, R. Watkins, and K. A. Olive, *Nucl. Phys.* **B310**, 693 (1988).
- [8] J. R. Ellis, J. S. Hagelin, D. V. Nanopoulos, K. A. Olive, and M. Srednicki, *Nucl. Phys.* **B238**, 453 (1984).
- [9] B. W. Lee and S. Weinberg, *Phys. Rev. Lett.* **39**, 165 (1977).
- [10] M. Pospelov, A. Ritz, and M. B. Voloshin, *Phys. Lett. B* **662**, 53 (2008).
- [11] X.-G. He, X.-D. Ma, and G. Valencia, *J. High Energy Phys.* 03 (2023) 037.
- [12] G. Li, T. Wang, J.-B. Zhang, and G.-L. Wang, *Eur. Phys. J. C* **81**, 564 (2021).
- [13] J. F. Kamenik and C. Smith, *J. High Energy Phys.* 03 (2012) 090.
- [14] B. Patt and F. Wilczek, [arXiv:hep-ph/0605188](https://arxiv.org/abs/hep-ph/0605188).
- [15] M. W. Winkler, *Phys. Rev. D* **99**, 015018 (2019).
- [16] G. Krnjaic, *Phys. Rev. D* **94**, 073009 (2016).
- [17] A. Filimonova, R. Schäfer, and S. Westhoff, *Phys. Rev. D* **101**, 095006 (2020).
- [18] A. Kachanovich, U. Nierste, and I. Nišandžić, *Eur. Phys. J. C* **80**, 669 (2020).
- [19] M. Ovchinnikov, M. A. Schmidt, and T. Schwetz, *Eur. Phys. J. C* **83**, 791 (2023).
- [20] P. Asadi, A. Bhattacharya, K. Fraser, S. Homiller, and A. Parikh, *J. High Energy Phys.* 10 (2023) 069.
- [21] P. Athron, R. Martinez, and C. Sierra, *J. High Energy Phys.* 02 (2024) 121.
- [22] K. Schmidt-Hoberg, F. Staub, and M. W. Winkler, *Phys. Lett. B* **727**, 506 (2013).
- [23] B. Batell, M. Pospelov, and A. Ritz, *Phys. Rev. D* **83**, 054005 (2011).
- [24] D. Bečirević, G. Piazza, and O. Sumensari, *Eur. Phys. J. C* **83**, 252 (2023).
- [25] C. Grunwald, G. Hiller, K. Kröninger, and L. Nollen, *J. High Energy Phys.* 11 (2023) 110.
- [26] D. McKeen, *Phys. Rev. D* **79**, 015007 (2009).
- [27] P. Gondolo and G. Gelmini, *Nucl. Phys.* **B360**, 145 (1991).
- [28] A. Alloul, N. D. Christensen, C. Degrande, C. Duhr, and B. Fuks, *Comput. Phys. Commun.* **185**, 2250 (2014).
- [29] G. Belanger, F. Boudjema, P. Brun, A. Pukhov, S. Rosier-Lees, P. Salati, and A. Semenov, *Comput. Phys. Commun.* **182**, 842 (2011).
- [30] M. Acciarri *et al.* (L3 Collaboration), *Phys. Lett. B* **385**, 454 (1996).
- [31] D. Foreman-Mackey, D. W. Hogg, D. Lang, and J. Goodman, *Publ. Astron. Soc. Pac.* **125**, 306 (2013).
- [32] N. Aghanim *et al.* (Planck Collaboration), *Astron. Astrophys.* **641**, A6 (2020); **652**, C4(E) (2021).
- [33] P. Agnes *et al.* (DarkSide Collaboration), *Phys. Rev. Lett.* **121**, 081307 (2018).
- [34] A. H. Abdelhameed *et al.* (CRESST Collaboration), *Phys. Rev. D* **100**, 102002 (2019).
- [35] C. Amole *et al.* (PICO Collaboration), *Phys. Rev. D* **100**, 022001 (2019).
- [36] Y. Meng *et al.* (PandaX-4T Collaboration), *Phys. Rev. Lett.* **127**, 261802 (2021).
- [37] E. Aprile *et al.* (XENON Collaboration), *Phys. Rev. Lett.* **121**, 111302 (2018).
- [38] A. Badin and A. A. Petrov, *Phys. Rev. D* **82**, 034005 (2010).
- [39] Y. Ku *et al.* (Belle Collaboration), *Phys. Rev. D* **102**, 012003 (2020).
- [40] R. L. Workman *et al.* (Particle Data Group), *Prog. Theor. Exp. Phys.* **2022**, 083C01 (2022).
- [41] G. Li, T. Wang, J.-B. Zhang, and G.-L. Wang, *Eur. Phys. J. C* **81**, 564 (2021).
- [42] F. Mescia and C. Smith, *Phys. Rev. D* **76**, 034017 (2007).
- [43] A. J. Buras, J. Harz, and M. A. Mojahed, [arXiv:2405.06742](https://arxiv.org/abs/2405.06742).
- [44] E. Cortina Gil *et al.* (NA62 Collaboration), *J. High Energy Phys.* 06 (2021) 093.
- [45] K. Schmidt-Hoberg, F. Staub, and M. W. Winkler, *Phys. Lett. B* **727**, 506 (2013).
- [46] G. Krnjaic, *Phys. Rev. D* **94**, 073009 (2016).
- [47] A. Fradette and M. Pospelov, *Phys. Rev. D* **96**, 075033 (2017).
- [48] S. Jia *et al.* (Belle Collaboration), *Phys. Rev. Lett.* **128**, 081804 (2022).
- [49] I. Adachi *et al.* (Belle-II Collaboration), *Phys. Rev. D* **108**, L111104 (2023).
- [50] S. Jia *et al.* (Belle Collaboration), *Phys. Rev. Lett.* **128**, 081804 (2022).
- [51] M. Ablikim *et al.* (BESIII Collaboration), *Phys. Rev. D* **105**, 012008 (2022).
- [52] R. Aaij *et al.* (LHCb Collaboration), *Phys. Rev. Lett.* **115**, 161802 (2015).
- [53] R. Aaij *et al.* (LHCb Collaboration), *Phys. Rev. D* **95**, 071101 (2017).
- [54] E. Cortina Gil *et al.* (NA62 Collaboration), *J. High Energy Phys.* 03 (2021) 058.
- [55] E. Cortina Gil *et al.* (NA62 Collaboration), *J. High Energy Phys.* 02 (2021) 201.
- [56] A. Alavi-Harati *et al.* (KTeV Collaboration), *Phys. Rev. Lett.* **93**, 021805 (2004).
- [57] E. Abouzaid *et al.* (KTeV Collaboration), *Phys. Rev. D* **77**, 112004 (2008).
- [58] J. D. Clarke, R. Foot, and R. R. Volkas, *J. High Energy Phys.* 02 (2014) 123.
- [59] F. Bezrukov and D. Gorbunov, *J. High Energy Phys.* 05 (2010) 010.
- [60] S. Alekhin *et al.*, *Rep. Prog. Phys.* **79**, 124201 (2016).
- [61] D. Gorbunov, I. Krasnov, and S. Suvorov, *Phys. Lett. B* **820**, 136524 (2021).
- [62] G. Elor, R. McGehee, and A. Pierce, *Phys. Rev. Lett.* **130**, 031803 (2023).
- [63] P. N. Bhattiprolu, G. Elor, R. McGehee, and A. Pierce, *J. High Energy Phys.* 01 (2023) 128.

- [64] W. G. Parrott, C. Bouchard, and C. T. H. Davies (HPQCD Collaboration), *Phys. Rev. D* **107**, 014510 (2023).
- [65] J. A. Bailey *et al.*, *Phys. Rev. D* **93**, 025026 (2016).
- [66] N. Gubernari, A. Kokulu, and D. van Dyk, *J. High Energy Phys.* **01** (2019) 150.
- [67] Y. Aoki *et al.* (Flavour Lattice Averaging Group (FLAG) Collaboration), *Eur. Phys. J. C* **82**, 869 (2022).
- [68] A. Bharucha, D. M. Straub, and R. Zwicky, *J. High Energy Phys.* **08** (2016) 098.